Available online at www.sciencedirect.com
SCIENCE DIRECT
Biochimica et Biophysica Acta 1669 (2005) 75–86
BIOCHIMICA ET BIOPHYSICA ACTA
BBA
http://www.elsevier.com/locate/bba

Environmental factors that enhance the action of the cell penetrating peptide pep-1 A spectroscopic study using lipidic vesicles

Sónia Troeira Henriques, Miguel A.R.B. Castanho*

Centro de Química e Bioquímica, Faculdade de Ciências da Universidade de Lisboa, Ed. C8, Campo Grande, 1749-016 Lisboa, Portugal

Received 2 September 2004; received in revised form 18 November 2004; accepted 19 November 2004
Available online 5 March 2005

Abstract

Pep-1 is a cell penetrating peptide (CPP) derived from the nuclear localization sequence of Simian Virus 40 large antigen T and from reverse transcriptase of Human Immunodeficiency Virus. Although it has been successfully used to transport proteins into cells, its action at the molecular level is not yet clear, mainly the local environmental factors that condition partition and translocation. Characterization in aqueous medium and quantification of partition into bilayers were carried out. Dynamic light scattering studies show that pep-1 self-associates in aqueous medium. The role of the bilayer phase, anionic lipids, ionic strength of the medium, reducing agents and pep-1 concentration on the extent and kinetics of partition were studied. Unlike others cationic CPP (e.g. penetratin) pep-1 has a high affinity to neutral vesicles ($K_p = 2.8 \times 10^3$), which is enhanced by anionic lipids. In a reduction environment partition is strongly inhibited ($K_p = 2.2 \times 10^2$), which might be a key-feature in the biological action of pep-1. Peptide incorporation takes place in the millisecond time-range to the lipidic interfaces. These environmental factors are systematized to enlighten how they help cellular uptake.

Keywords: Translocation; Vector; Peptide carrier; Fluorescence; Vesicle

1. Introduction

The observation that some intracellular proteins translocate naturally across the plasmatic membrane and the identification of basic peptidic sequences responsible for this ability, lead to novel techniques of protein transduction [1–6]. These peptidic sequences, also known as protein transduction domains (PTDs), have been used and optimized as carriers. The three most investigated PTDs are derived from the Human Immunodeficiency Virus 1 (HIV-1) transcriptional activator (tat), the *Drosophila* homeotic transcription factor Antennapedia (Antp), and the Herpes Simplex Virus (HSV) protein VP22 [1,2,5,7]. These PTDs require covalent coupling with the target protein [3,7]. However, this kind of interaction induces alterations in the native form of protein, which can limit the technology [7].

Pep-1 is a synthetic peptide carrier forming non-covalent hydrophobic interactions with the cargo, capable of introducing a great variety of proteins in different cellular lines, without the need to denature proteins [7–10]. This kind of interaction stabilizes the protein, avoiding degradation and preserving its natural characteristics [7,9]. Pep-1 delivers proteins into mammalian cells [7,8,10–12], or in plant cells converted in protoplasts [13], and maintains at least 80% of the viability of different cellular cultures in concentrations up to 1 mM [7] at an average efficiency of 60–95%, depending on the cell type and the protein being transduced [8]. Since it is a non-toxic and non-invasive method with results in less than 2 h, pep-1 is an attractive vehicle to introduce functional proteins in cells [7,8]. This method can potentially: 1) correct genetic diseases by altering the phenotype; 2) function like a vaccine by the introduction of antibodies and 3) be used for research on the study of the function/structure of proteins.

* Corresponding author. Tel.: +351 217500931; fax: +351 217500088.
E-mail address: castanho@fc.ul.pt (M.A.R.B. Castanho).

0005-2736/$ - see front matter © 2005 Elsevier B.V. All rights reserved.
doi:10.1016/j.bbamem.2004.11.017

Pep-1 has 21 amino acids residues (KETWWETWWTEWSQPKKKRKV) with three different domains: the so-called hydrophobic, rich in Trp residues (KETWWETWWTEW), the hydrophilic one rich in basic amino acids (KKKRKV) and a spacer sequence with a Pro (SQP), between the other two [7]. The peptide is acetylated in the N terminal and has a cysteamine group on the C terminal [7] and has a tendency to form disulfide bonds in aqueous solution. The hydrophobic domain is from HIV-1 reverse transcriptase [14] and is responsible for both forming hydrophobic interactions with proteins and for an efficient targeting to the cell membrane [7]. The hydrophilic sequence is a nuclear localization signal (NLS) from the large antigen T of Simian Virus 40 (SV40) [7] and has been used in other peptide carriers [9,15]. This domain improves solubility and intracellular distribution of the peptide [7]. The presence of the Pro residue in spacer sequence promotes a large flexibility and the integrity of other two domains [7].

The understanding of the mechanism of Pep-1 action and the local environmental factors that affect such a mechanism is of first importance for a generalized application and optimization of the process. The amphipaticity of the carrier suggests a strong interaction with the lipidic biomembranes. Despite some molecular-level details, biochemical and biophysical actions of pep-1 are still unknown; Silvius and co-workers recently demonstrated that translocation of cell penetrating peptides is intimately related to the transmembrane potential across lipidic membranes [16]. For pep-1, dependence on membrane potential for translocation occurrence was also verified [17]. Deshayes et al. [18] addressed several specific points relative to pep-1 translocation. Our aim in this paper is to give insight on additional environmental processes that furthermore favour translocation. The presence of five residues of Trp enables the application of fluorescence spectroscopy techniques with no need for derivatization with a fluorescent probe.

2. Material and methods

2.1. Materials

Chariot™, the commercial name of pep-1, was obtained from Active Motif (Rixensart, Belgium) with purity higher than 95%, carboxyfluorescein-labelled pep-1 (pep-1-CF; linked by a Lys in C terminal and blocked with a Ser) was obtained from GenScript Corporation (Piscataway, New Jersey) with purity higher than 95%; 2-(4-(2-Hydroxyethul)-1-piperazinyl) ethanesulfonic acid (HEPES), sodium chloride, L-Tryptophan, acrylamide, ethanol and chloroform spectroscopic were from Merk (Darmstadt, Germany); 1-Palmitoyl-2-Oleoyl-*sn*-Glycero-3-Phosphocholine (POPC), 1-Palmitoyl-2-Oleoyl-*sn*-Glycero-3-(Phospho-rac-(1-glycerol)) (POPG), 1,2-Dipalmitoyl-*sn*-Glycero-3-phosphocholine (DPPC) and 1,2-Dipalmitoyl-*sn*-Glycero-3-(phospho-L-serine) (DPPS), from Avanti Polar-Lipids (Alabaster, Alabama); 5-Doxyl-stearic acid (5DS) and 16-Doxyl-stearic acid (16DS) from Aldrich Chem Co. (Milwaukee, Wisconsin); Cholesterol (chol) and DL-Dithiothreitol (DTT) from sigma (St. Louis, Missouri), *tris*-(2-cyanoethyl)phosphine (phosphine) from molecular probes (Eugene, Oregon), and Oxidized glutathione (GSSG) from Boehringer Manheim (Germany).

Pep-1 solutions were prepared in HEPES buffer (10 mM HEPES, pH 7.4 containing 10 mM (low ionic strength) or 150 mM NaCl (the so-called physiologic ionic strength)). The assays were performed at room temperature in a UV-Vis spectrophotometer Jasco V-530 and in a spectrofluorometer SLM Aminco 8100, equipped with 450 W Xe lamp, Glan-Thompson polarizers, and double monochromators. Fluorescence intensity values were corrected for inner filter effect [19].

2.2. Characterization of pep-1 in aqueous solution

Spectral characterization was performed and fluorescence steady-state anisotropy was used to study red-edge effects (details have been published elsewhere, see Ref. [20]). Quantum yield-dependence on peptide concentration, ionic strength and reduction effects in the presence of phosphine (1 mM) were also evaluated.

A light scattering apparatus equipped with a He–Ne laser (632.8 nm; 35 mW) model 127 from Spectra-Physics and a 72 channels UNICOR autocorrelator was used to study the aggregation of pep-1 in aqueous solution. Peptide solutions were filtered through a sterile 0.22 μM pore Millipore filter. Data was fitted with a tri-exponential function; the average diffusion coefficient, D, was determined (λ=632.8 nm; right angle geometry) and hydrodynamic radius, R_h, was calculated by means of the Stokes–Einstein equation (details have been published elsewhere, see Ref. [21]).

Pep-1-CF solutions (0.023, 0.058, 0.12, 0.17, 0.23 and 0.58 μM) at low ionic strength, were titrated with small volumes of a pep-1 stock solution (688 μM). Pep-1-CF fluorescence was followed with λ_{exc}=490 nm.

2.3. Reduction effect and fluorescence quenching in aqueous solution

Quenching assays were followed by fluorescence intensity with excitation at 280 nm and emission at 350 nm unless stated otherwise. Fluorescence quenching by acrylamide was carried out using λ_{exc}=290 nm to minimize the relative quencher/fluorophore light absorption ratio. Nevertheless, the quenching data were corrected for the simultaneous light absorption of fluorophore and quencher [22]. Quenching assays data with negative deviation from the Stern–Volmer representation Eq. (1) were analysed using Eq. (2),

$$\frac{I_0}{I} = 1 + K_{SV}[Q] \quad (1)$$

(I and I_0 are the fluorescence intensity of the sample in the presence and absence of quencher, respectively, K_{SV} is the Stern–Volmer constant and $[Q]$ the concentration of quencher) [20,23],

$$\frac{I_0}{I} = \frac{1 + K_{SV}[Q]}{(1 + K_{SV}[Q])(1 - f_B) + f_B} \quad (2)$$

($f_B = \frac{I_{0,B}}{I_0}$ is the fraction of light accessible to the quencher and $I_{0,B}$ is the fluorescence intensity of the accessible population to the quencher, when $[Q]=0$ [20,23]).

2.4. Preparation of lipid vesicles

Large unilamellar vesicles (LUVs), with typical 100 nm diameter [24] were prepared by the extrusion method described elsewhere [25] and used as models of biological membranes.

2.5. Extent and kinetics of partition in LUV

The extent and kinetics of partition assays of pep-1 (6.88 μM) in the absence or presence of phosphine (1 mM), were carried out with LUVs of POPC and POPG (liquid-crystal phase), DPPC and DPPS (gel phase) or POPC and chol (2:1) (liquid-ordered phase). Titrations of pep-1 with lipidic suspensions (final concentrations ranges from 0 to 3.75 mM), both in low and physiologic ionic strength, were used to evaluate the extent of the partition. Samples were left to incubate for 10 min after each addition of lipid suspension. The partition coefficient, K_p, is calculated from the fit of experimental data with Eq. (3) as described elsewhere [26]

$$\frac{I}{I_W} = \frac{1 + K_p\gamma_L \frac{I_L}{I_W}[L]}{1 + K_p\gamma_L[L]} \quad (3)$$

where I_W and I_L are the fluorescence intensities in aqueous solution and in lipid solution, respectively, γ_L is the molar volume of lipid and $[L]$ is the lipidic concentration) [26] γ_L used was 7.63×10^{-1} dm^3 mol^{-1} for vesicles containing POPC [27] and 6.89×10^{-1} dm^3 mol^{-1} for vesicles containing DPPC [28]. Pep-1 is restricted to the outer leaflet of bilayers in the absence of a transbilayer potential [17], so data analysis was carried out considering the effective lipid concentration as half of the total lipid concentration [26].

Kinetic assays were followed by fluorescence emission intensity (λ_{ex}=280 nm and λ_{em}=340 nm; pep-1 in lipidic vesicles has a 10 nm blue-shifted emission spectrum, by application of Eq. (AI.8), see Appendix B). Lipidic suspensions (final concentration of 3.75 mM; this concentration ensures that the molar fraction of partitioned peptide in lipidic phase, X_L, is ≥0.8, calculated using Eq. (4) [29]) were added to the peptide solutions (6.88 μM) with physiologic ionic strength.

$$X_L = \frac{K_p\gamma_L[L]}{1 + K_p\gamma_L[L]} \quad (4)$$

The Eq. (AIII.11) deduced in Appendix C was used to fit the kinetics data.

2.6. Location in lipidic membranes

The membrane in-depth location of the pep-1 Trp residues was studied by differential quenching methodologies. 5DS and 16DS are quenchers of Trp fluorescence, which have different locations in the lipidic bilayer. 5DS is located near the interface while 16DS buries more deeply into the bilayer core [30]. Titration of peptide samples (6.88 and 1.45 μM), in the presence of LUVs composed of different lipid mixtures (3.5 mM lipid in buffer with low or physiologic ionic strength), was carried out with ethanolic solution of 5DS and 16DS (final ethanol concentration was kept below 2%). The assays were followed by fluorescence emission intensity (λ_{ex}=280 nm, λ_{em}=340 nm). Data were corrected for simultaneous absorption of fluorophore and quencher [22]. Effective concentration of quencher in the lipidic bilayer matrix, $[Q]_L$,

$$[Q]_L \approx \frac{K_{p,Q}[Q]_T}{1 + K_{p,q}\gamma_L[L]} \qquad \gamma_L[L] \ll 1 \quad (5)$$

was used in the Stern–Volmer plots; $[Q]_T$ is the quencher concentration in total solution volume and $K_{p,Q}$ is the quencher partition coefficient [29]. For gel phase vesicles $K_{p,Q}$ equals 12,570 and 3340 for 5 DS and 16 DS, respectively. In crystal-liquid-like phase the values used for 5 DS and 16 DS were 89,000 and 9730, respectively [31].

Acrylamide is unable to efficiently quench the fluorescence of Trp residues deeply buried in the bilayer; titration of peptide in the presence of LUVs with this quencher also gives insight on peptide in-depth location [19]. Fluorescence emission quenching (λ_{exc}=290 nm, λ_{em}=340 nm) with acrylamide was carried out with different lipidic mixtures (3.5 mM lipid concentration) in the absence and presence of phosphine (1 mM).

3. Results and discussion

3.1. Aqueous solution

The organization of pep-1 may be potentially influenced by the ionic strength (pep-1 is a charged peptide at pH 7.4) and reduction agents (via inter-molecular disulfide bonds at the cysteamine terminal). Pep-1 has five Trp residues located in its so-called hydrophobic region, which enable structural characterization by fluorescence spectroscopy. The fluorescence spectra of peptide and free Trp in aqueous media present equal vibrational progression (Fig. 1A), this is true both in low and physiologic ionic strength.

At low ionic strength the peptide quantum yield is slightly concentration-dependent (Fig. 1B). Dynamic light scattering correlograms (data not shown) show evidence for the presence of aggregates with mean (weight-averaged) hydro-

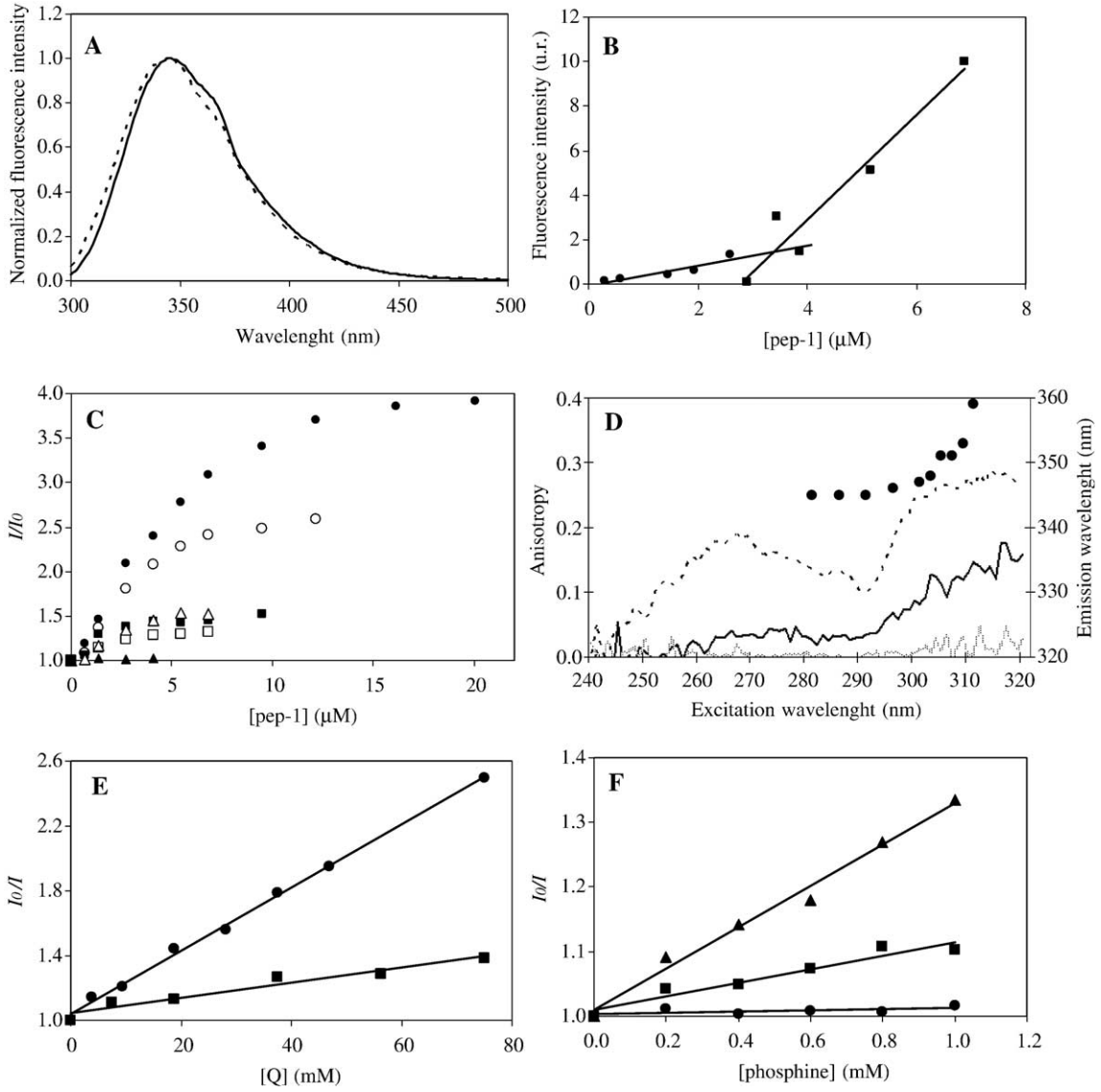

Fig. 1. Characterization of Pep-1 in aqueous solution. Pep-1 (or free Trp) in 10 mM HEPES buffer pH 7.4 containing 10 mM NaCl. (A) Fluorescence emission spectra (λ_{exc}=280 nm) of free Trp (solid line) and pep-1 (dashes) in aqueous solution. (B) Fluorescence intensity (λ_{exc}=280 nm and λ_{em}=350 nm) dependence on pep-1 concentration. There are two linear zones with different slopes, that intersect at an apparent critical concentration (3.4 ± 1.7 μM); below (circles) and above (squares) it, the peptide has different quantum yields. (C) Titration of 0.023 (solid circle), 0.058 (open circles), 0.12 (solid square), 0.17 (open square), 0.23 (open triangle) and 0.58 μM (solid triangle) pep-1-CF with non-labelled pep-1 followed by fluorescence emission at λ_{exc}=490 nm λ_{em}=520 nm. (D) Red-edge excitation shift of 6.88 μM pep-1: variation of maximum emission wavelength (circles) and variation of anisotropy for pep-1 (black solid line), free Trp in buffer (control 1; grey solid line) and free Trp in glycerol (control 2; dashes) with the excitation wavelength. (E) Quenching of fluorescence emission of free Trp by GSSG (circles) and by GSH (squares), notice that hydrolysis of one GSSG molecule forms two GSH molecules. (F) Effect of reducing agent phosphine on free Trp (control; circles), 6.88 μM pep-1 (squares) and 1.45 μM pep-1 (triangles).

dynamic radius of $<R_h>$ ≈ 60 nm in both 1.45 μM and 6.88 μM pep-1 solutions (i.e. below and above the apparent critical concentrations of 3.4 ± 1.7 μM (Fig. 1B)). However these averaged values do not exclude the presence of smaller aggregates in suspension (light scattering techniques have very low sensitivity for smaller aggregates in polydispersed systems) [32]. It is not possible to conclude from Fig. 1B alone if the "critical concentration" is a monomer/micelle transition or reflects the clustering of previously formed n-mers (similarly to what was concluded for polyene antibiotics [33]). Fig. 1C shows that, when pep-1-CF is titrated with unlabelled peptide, fluorescence emission intensity of the carboxy-fluorescein moiety increases when low concentrations of labelled peptide are used. This may be explained on the basis of fluorescence re-absorption ("trivial effect" energy transfer) caused by self-aggregation and closely packed chromophores. Trapping photons in the oligomers increase the probability of non-radiative decay of the fluorophores to the ground state. Therefore, oligomeric forms of the amphipathic peptide occur in solution.

Non-linear Stern–Volmer plots for the fluorescence quenching of the aggregates by the hydrophilic molecule

acrylamide (f_B=0.59 and 0.61 for 1.45 and 6.88 μM, respectively) are evidence that Trp residues sense heterogeneous local micro-environments [26]. Moreover, there is a fraction of the fluorophores not in contact with the aqueous solvent (hydrophobic "pockets" in the aggregates). This result is further confirmed by the occurrence of red-edge excitation shift in the fluorescence spectra of 6.88 μM pep-1 (Fig. 1D), which supports the hypothesis of a reduced mobility on the Trp side chain [34]. A complete depolarization of clustered pep-1 at $\lambda_{excitation}$<280 nm at variance to what is observed with immobilized Trp residues in glycerol (Fig. 1D) is a consequence of Trp–Trp energy migration (homotransfer), which is favoured by adjacent Trp residues in the peptide sequence. Energy migration is known to play a role in red-edge phenomena since red-shifting of Trp emission leads to a decrease in the absorption/emission spectral overlap [23]. Depolarization by migration is not efficient and anisotropy raises at the red-edge. The large ratio of anisotropies taken at 310/270 nm is a consequence of energy migration. Largely shifted emission spectra of Trp (Fig. 1D) are not common but other cases have been reported before [26,35].

It should be stressed that -SH group is a quencher of Trp fluorescence (Fig. 1E). Moreover disulfide bonds are also efficient quenchers (Fig. 1E). The differential effect of the reducing agent phosphine on the fluorescence quantum yield of the aggregates below and above the apparent critical concentration (Fig. 1F) is an evidence of an alteration of the internal molecular structure of the aggregate. Reduction of the -S-S- bonds implies a more pronounced effect at lower concentration (quenching is enhanced with the addition of phosphine; reduction of -S-S- induces a larger diffusional freedom of pep-1, resulting in improved quenching of Trp residues by -SH groups). At higher concentrations, the addition of phosphine does not induce a pronounced alteration in the contact of -S-S- or -SH groups with Trp residues. The fraction of fluorophores accessible to acrylamide in the presence of reducing agent phosphine is bigger for 1.45 μM pep-1 (f_B=0.80) than for 6.88 μM (f_B=0.71). The red-edge excitation shift for 6.88 μM pep-1 is not significantly influenced by the reducing agent phosphine.

At physiologic ionic strength the pep-1 quantum yield is independent of concentration and is not altered in the presence of reducing agent (data not shown). These results suggest that the organization of pep-1 is similar in the range of concentrations evaluated. A non-linear Stern–Volmer (f_B=0.73 for 1.45 μM and 0.63 for 6.88 μM pep-1) and a red-edge excitation shift was also observed for physiologic ionic strength, indicating that peptide aggregates in aqueous solution, but organization of these aggregates is not dependent on concentration.

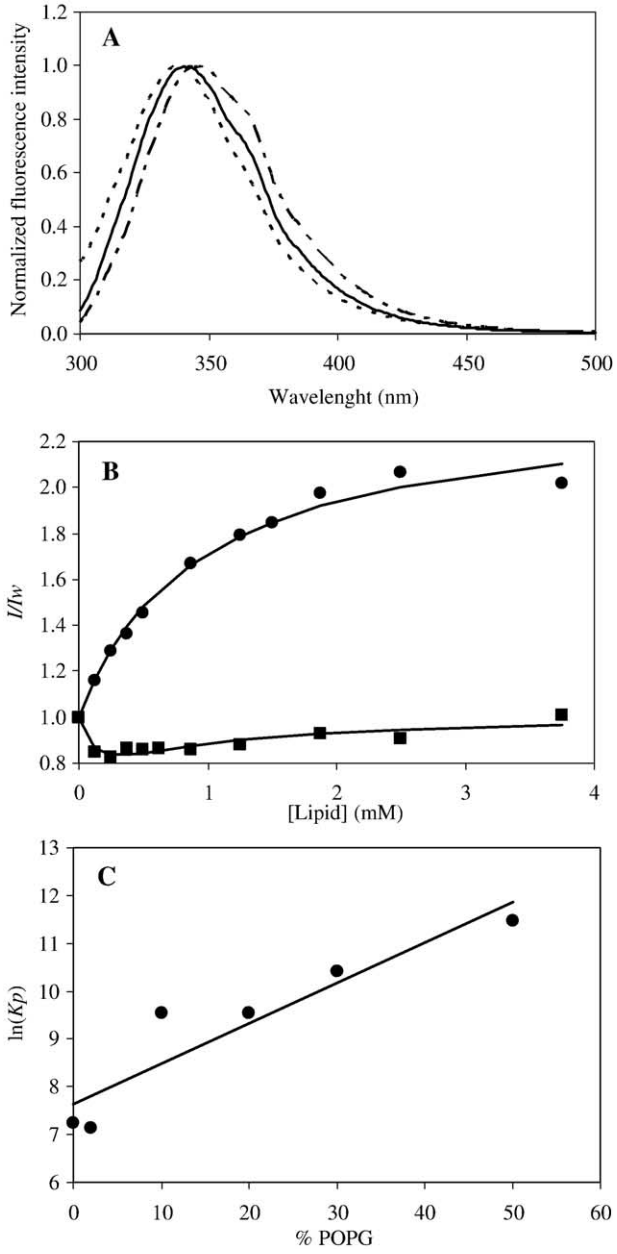

Fig. 2. Partition of pep-1 in LUVs. 6.88 μM pep-1 in 10 mM HEPES buffer pH 7.4 containing 10 mM NaCl. (A) Fluorescence emission spectra of pep-1 in aqueous solution (long and short dashes), in the presence of 0.5 mM POPC LUVs (solid line) and when is completely inserted in lipidic phase (short dashes; spectra calculated using Eq. (AI.8), Appendix A); fluorescence emission spectra were recorded for other lipidic concentrations but only one is represented for the sake of simplicity. (B) Fluorescence emission intensity of pep-1 normalized to [L]=0 (I/I_W) upon titration with LUVs of POPC (circles) or DPPC (squares)—Eq. (3) and Eq. (AII.10) (see Appendix B), respectively, were fitted to data. (C) K_p (logarithmic scale) of pep-1 in vesicles with different molar ratios of POPC:POPG.

3.2. Extent of partition into liquid-crystal bilayers

Titration of aqueous suspensions of the peptide (1.45 or 6.88 μM) with lipidic vesicles leads to blue-shifted emission spectra (Fig. 2A) and an increase in the fluorophore quantum yield (Fig. 2B). The fluorescence intensity is related to K_p by Eq. (3). When POPC large unilamellar vesicles are used ([pep-1]=6.88 μM), $K_p=(2.8\pm0.6)\times10^3$ for low ionic strength, which leads to $\Delta G=-1.9\times10^4$ J mol^{-1}. The calculated molar fraction of the peptides

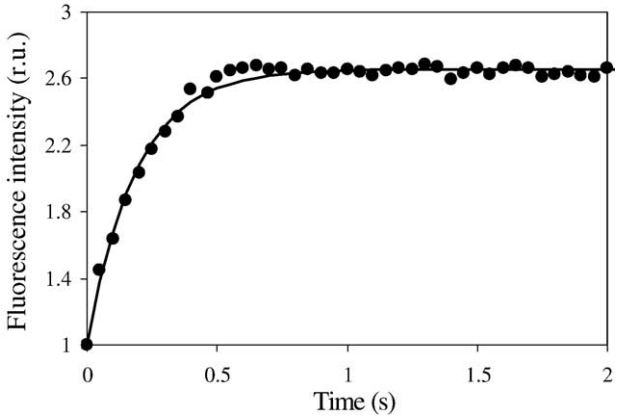

Fig. 3. Partition kinetics of 6.88 μM pep-1 (10 mM HEPES buffer pH 7.4 containing 150 mM NaCl) in 3.75 mM DPPC:DPPS (4:1) LUVs. Fit was realized with Eq. (A.III.11) (see Appendix C).

inserted in the lipidic matrix at 3.5 mM POPC (close to the reference value in biological systems [36]) is X_L=0.80 (Eq. (4)). This value is not sensitive to the ionic strength of the medium (K_p=(3.4 ± 0.6) × 10^3 for physiologic strength), because POPC is globally a neutral lipid. K_p increases exponentially with the molar fraction content of the negatively charged lipid POPG in the POPC bilayer (Fig. 2C). Such exponential behaviour is predicted under the framework of simple theories [37]. For 20% negative lipids (the expected natural occurrence in most cells [38]) and [L]=3.5 mM, X_L is very close to 100% (K_p=2.8 ± 0.4) × 10^4), i.e. virtually all the peptide is inserted in biological membranes. Naturally, at higher ionic strengths, partition coefficient values are decreased (K_p=2.2 ± 0.4) × 10^4), but the difference is not significant and for [L]=3.5 mM X_L is also close to 100%. When phosphine is added to the POPC suspension, K_p is remarkably reduced to (4.8 ± 1.2) × 10^2, showing that the aggregate formed by monomeric peptides in aqueous solution is more stable than the aggregates formed by the dimers. In other words, the reducing environment stabilizes the peptide in aqueous solution. A similar phenomenon was reported for a magainin analogue [39]. When POPG (20%) is present, K_p is also decreased in reducing conditions ((7.2 ± 2.4) × 10^2 for physiologic ionic strength), which means that peptide organization effects superimpose to electrostatic ones in partition.

3.3. Extent of partition into gel phase bilayers

The importance of biomembranes lateral heterogeneity (membrane domains) in the occurrence and control of several biochemical phenomena [40] prompted us to study gel-phase membranes in addition to fluid liquid-crystal ones. DPPC, a neutral lipid at pH 7.4, forms gel bilayers in aqueous environment at room temperature. In the presence of DPPC, the fluorescence spectrum of the peptide is blue-shifted relative to aqueous solution (data not shown). Nevertheless, the fluorescence quantum yield decreases at low lipid concentrations, increasing afterwards (Fig. 2B). We explored the hypothesis that this could be due to self-quenching because at low lipidic concentrations the peptide/lipid molar ratio is high. Eq. (AII.10) was derived (see Appendix B) assuming self-quenching occurrence in partition plots and it fits the experimental data (Fig. 2B). There is no significant difference in partition coefficients of [pep-1]=6.88 μM, for low and physiologic ionic strength (K_p=(1.3 ± 0.4) × 10^4 and (0.6 ± 0.2) × 10^4, respectively). As partition to gel phase bilayers occurs as surface adsorption and/or insertion in line defects in the lipidic palisades, a direct and quantitative comparison with K_p obtained in POPC is prevented. Yet, it should be stressed that K_p is also quite big in rigid lipidic areas of heterogeneous membranes. As before, in the presence of phosphine K_p decreases at both ionic strength ((8.0 ± 1.6) × 10^3 for low ionic strength and (8.0 ± 2.3) × 10^3 for physiologic ionic strength). DPPS, a negatively charged lipid which keeps gel phase properties in the DPPC matrix, causes an increase in K_p up to 10% molar (K_p=(1.4 ± 0.6) × 10^5 for low ionic strength). In the 10–50% range K_p is broadly constant (data not shown). This saturation is probably related to a saturation of the line defects in the gel. Likewise, increasingly blue-shifted emission fluorescence spectra are observed up to 5% DPPS, the wavelength of the emission maximum remaining constant after that.

3.4. Extent of partition into cholesterol-containing bilayers

POPC bilayers having 33% molar cholesterol are homogeneous [41] and can be regarded as model compositions to study liquid-ordered-like patches in biological membranes [42]. Both blue-shifted emission spectra and increased fluorescence quantum yield are detected when pep-1 is in the presence of POPC/cholesterol vesicles. Evidence for self-quenching at high peptide/lipid ratios is obtained (data not shown), as before with DPPC. Nevertheless, the apparent extent of partition is close to the one measured when only POPC was used, (K_p=(3.4 ± 0.4) × 10^3 for low ionic strength and (2.2 ± 0.6) × 10^3 for physiologic ionic strength). Cholesterol affects the partition patterns but not significantly its extent i.e. it favours sulfur/indole interactions, whether by modulation of its organ-

Table 1
Parameters of 6.88 μM pep-1 kinetic incorporation in LUVs, determined by non-linear regression fitting of Eq. (AIII.11) (see Appendix C)

Lipid[a]	$t_{1/2}$ (× 10^2 ms)	K_p (× 10^4)
POPC	6.9 ± 5.2	1.2 ± 0.7
POPC:POPG (4:1)	0.5 ± 0.3	3.4 ± 1.8
POPC:col (2:1)	1.9 ± 0.3	1.5 ± 0.5
DPPC	2.4 ± 0.8	1.4 ± 0.4
DPPC:DPPS (4:1)	1.2 ± 0.3	2.6 ± 0.6

[a] The final lipidic concentration in each case is 3.75 mM (10 mM HEPES buffer pH 7.4 containing 150 mM NaCl).

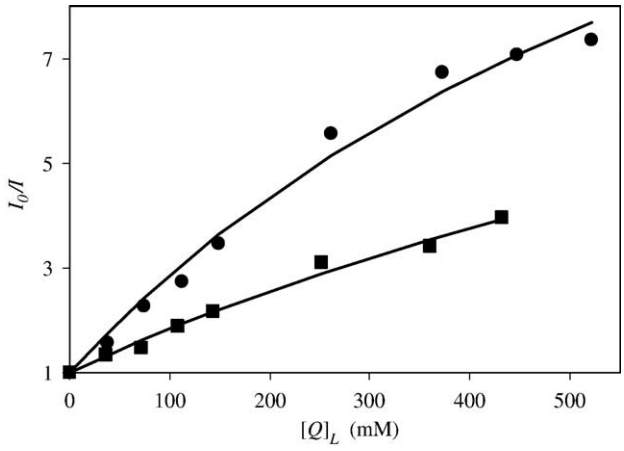

Fig. 4. Pep-1 location in POPC LUVs. Stern–Volmer plot of the fluorescence quenching of 6.88 μM Pep-1 by 5DS (circles) and 16DS (squares) concentration. Effective quencher concentration in lipidic phase was determined using Eq. (5). Eq. (2) was fitted to data by means of non-linear regression. Lipidic concentration is 3.5 mM in a 10 mM HEPES buffer pH 7.4 containing 10 mM NaCl.

ization, or by forcing peptide location in a narrower space of the membrane. The second hypothesis seems more reasonable, on the account of the results obtained with DPPC.

3.5. Kinetics

Partition of pep-1 into lipid bilayers occurs in the second time range, presenting an hyperbolic-like dependence of fluorescence intensity with time (Fig. 3).This dependence was rationalized in terms of a simple partition model (Appendix C) and $t_{1/2}=\ln 2/k_{in}$, as well as K_p, were calculated by fitting Eq. (AIII.11) to the experimental data (Table 1). Partition is faster for gel-phase and liquid-ordered membranes relative to liquid-crystal ones. Anionic lipids decrease $t_{1/2}$. There is a correlation between partition extent and velocity. In spite of differences in methodologies to determine the K_p's, the ones obtained from kinetic data are in fair agreement with those obtained in steady-state experiments (the effect of negative lipids is well pronounced).

Table 3
Emission fluorescence quenching of 6.88 μM pep-1, incorporated in LUVs, by acrylamide[a]

Lipid	[phosphine] (mM)	K_{SV} (M^{-1})
POPC	0	3.1 ± 0.5
	1	17 ± 4.5
POPC:POPG (4:1)	0	2.7 ± 0.4
	1	30.9 ± 9.9
DPPC	0	3.1 ± 0.2
	1	69.4 ± 16.2
DPPC:DPPS (4:1)	0	3.8 ± 0.2
	1	19.3 ± 3.5

[a] Total lipidic concentration was 3.5 mM. Assays were performed in 150 mM (the so-called physiologic ionic strength) NaCl. f_B and K_{SV} were determined by fitting Eq. (2) to experimental data.

3.6. Pep-1 location in the lipid palisade

In-depth location on the pep-1 Trp residues was carried out by means of fluorescence quenching with doxyl derivatized stearic acid. The closer the Trp residues are to the quencher group, the more efficient is the quenching. Thus 5DS probes the bilayer interface while 16DS probes its core. More refined methods [30] are difficult to apply because the Trp residues span a 9-amino acids sequence in the peptide. Stern–Volmer plots show downward deviation from linearity (Fig. 4). This can be due to the existence of fluorescence sub-populations with differential accessibility to the quencher [23]. In the limit, a fraction of the fluorophores may be completely segregated from the quenchers [43]. For instance incomplete partition into membranes ($X_L<1$) renders a fraction of fluorophores completely inaccessible to lipophilic quenchers. Thus, Eq. (2) was used for data analysis. f_B should be equal to the fraction of light emitted from the incorporated peptide, f_L, which can be calculated from K_p [29]

$$f_L = \frac{(I_L/I_W)K_p\gamma_L[L]}{1+(I_L/I_W)K_p\gamma_L[L]} \quad (6)$$

The results are presented in Table 2. Regardless of the lipidic systems or peptide concentrations, 5DS is a more efficient quencher than 16DS. This is evidence of a shallow position of the so-called hydrophobic region of

Table 2
Emission fluorescence quenching of pep-1, incorporated in LUVs, by 5DS and 16DS[a]

[pep-1] (μM)	Lipid	Ionic strength	f_L	$f_{B,5DS}$	$K_{SV,5DS}$ (M^{-1})	$f_{B,16DS}$	$K_{SV,16DS}$ (M^{-1})
6.88	POPC	low	0.90	0.95 ± 0.43	22.1 ± 2.6	0.92 ± 0.45	9.7 ± 1.1
		physiologic	0.94	1	12.3 ± 0.5	1	3.6 ± 0.1
	POPC:POPG (4:1)	physiologic	0.99	0.96 ± 0.24	29.4 ± 1.9	1	6.3 ± 0.1
	DPPC	low	0.94	0.95 ± 0.22	70.4 ± 6.3	1	15.7 ± 0.4
		physiologic	0.98*	0.97 ± 0.30	207 ± 28	1	16.5 ± 0.7
	DPPC:DPPS (4:1)	physiologic	0.99*	0.92 ± 0.33	374 ± 61	1	8.8 ± 0.4
1.45	POPC	physiologic	0.95*	0.74 ± 0.24	27.2 ± 3.8	1	3.0 ± 0.1
	POPC:POPG (4:1)	physiologic	0.98*	0.78 ± 0.33	29.9 ± 5.2	1	6.3 ± 0. 4
	DPPC:DPPS (4:1)	physiologic	0.99*	0.81 ± 0.45	262 ± 67.9	0.77 ± 0.20	22.4 ± 2.4

[a] Total lipidic concentration was 3.5 mM. Assays were performed in 10 mM HEPES buffer containing 10 mM (low ionic strength) or 150 mM (the so-called physiologic ionic strength) NaCl. f_B and K_{SV} were determined by fitting Eq. (2) or Eq. (1) (f_B=1) to experimental data. f_L was determined by application of Eq. (6) using K_p values obtained by the steady-state or kinetic methodologies (marked with *).

pep-1 at the membrane interface. f_L is in agreement with $f_{B,5DS}$ and $f_{B,16DS}$, given the intrinsic experimental error. It is interesting to notice that the quenching efficiency using lipophilic doxyl probes is bigger in gel-phase membranes. This may be due to segregation of both fluorophore and quenchers to defect lines in the gel matrix, favouring static quenching mechanisms at high local concentrations in a molecular scale.

To further search the membrane insertion extent of pep-1, fluorescence quenching experiments using the hydrophilic quencher acrylamide were carried out at 6.88 μM pep-1 and 150 mM NaCl. Results presented in Table 3 demonstrate that fluorescence emission of pep-1 in the presence of LUVs is not efficiently quenched by acrylamide. Although Trp residues are located near the water–lipid interface, they are protected from aqueous environment. In the presence of a reducing agent the quenching efficiency was markedly improved, which suggests that pep-1 is not so extensively incorporated in lipidic vesicles. These results are in agreement with partition data.

4. Conclusions

In a recently published work [17] the capacity of pep-1 to translocate across a lipidic bilayer was demonstrated. Translocation in vesicles only occurs in the presence of a transmembrane potential. The nature of cell membrane (negatively charged inside and neutral outside) prompted us to evaluate the pep-1 affinity for lipidic bilayers in different conditions. The information gathered in the present study highlights some important features of environmental factors that may be crucial to pep-1 molecular action at the biological membrane level. Fig. 5 gathers the information into a mechanistic model. Most biomembranes are asymmetrically charged (neutral at the outer surface and negative inside [38]). The present study shows that Pep-1 in the outer aqueous environment inserts extensively into membranes, whether at high or low concentration, even when no transbilayer potential is present. After anchorage at the bilayer surface, electrostatic attraction combined with lipid bilayer perturbation probably causes translocation into the inner leaflet of the membrane [17]. Being an anionic interface, the release into the cellular environment could be problematic if it was not for the pep-1 reduction (Fig. 5), which turns the peptide aggregates into stable structures with low K_p. This makes the process irreversible in practice inside cells and pep-1 is then available for uptake by cellular compartments.

Results obtained with DPPC suggest that the liquid heterogeneity boundaries in biological membranes may serve as gateways for pep-1 crossing. Membrane fusion may also facilitate translocation, as addressed by Terrone et al. (2003) [16].

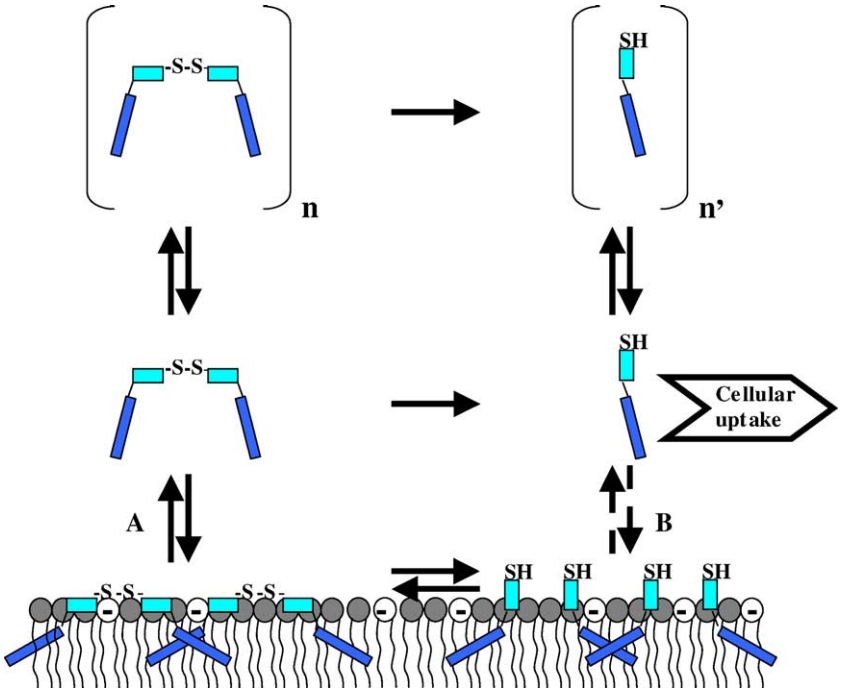

Fig. 5. Mechanistic model for the environmental factors that lead to cellular uptake of pep-1. Pep-1 in the outer aqueous environment incorporates extensively in lipidic bilayers (see text) and translocation occurs, mainly due to membrane perturbation and electrostatic interaction [17]. This sketch depicts the influence of a reducing environment at the cell interior, which is responsible for membrane detachment of pep-1 (thus, it is a crucial factor in pep-1 functionality). Although partition equilibrium of the dimerized peptide to the negatively charged inner leaflet of the mammals' model membranes (A) greatly favours lipidic phase (see text), reduction of pep-1 in the cell interior combined with a partition equilibrium (B) which favours aqueous phase for the monomeric peptide (see text) results in availability of free pep-1 inside the cell. Light blue fragments represent the Lys-rich hydrophilic domain. In dark blue are the Trp-rich domains.

Acknowledgements

We thank Drs. Manuel L. M. Lopes and Lara Penedo for helping with the dynamic light scattering, and Dr. Manuel Prieto (UTL, Portugal) for valuable discussions. Fundação para a Ciência e Tecnologia is acknowledged for funding and a grant to S. T. Henriques.

Appendix A. Theoretical calculation of the peptide fluorescence emission spectrum when it is completely inserted in lipid bilayers

The Trp emission fluorescence is very sensitive to the polarity of the surrounding solvent. The total emission spectrum of pep-1, $I_t(\lambda)$, is dependent both on the spectrum of pep-1 sub-population incorporated in lipid, $I_L(\lambda)$, and the spectrum of the sub-population of the fluorophore present in aqueous solution, $I_W(\lambda)$,

$$I_t(\lambda) = n_L i_L(\lambda) + n_W i_W(\lambda) = I_L(\lambda) + I_W(\lambda) \quad \text{(AI.1)}$$

where $i_i(\lambda)$ is the spectrum of one molecule and n_i the number of molecules in lipid, L, or in water, W. Eq. (AI.1) can be rewritten,

$$I_t(\lambda) = n_L \Phi_L I_{L,N}(\lambda) + n_W \Phi_W I_{W,N}(\lambda) \quad \text{(AI.2)}$$

where $I_{i,N}(\lambda)$ is the normalized emission spectrum; Φ_L and Φ_W are the quantum yield in lipid and water, respectively. Eq. (AI.2) can be rewritten in terms of the molar fraction of peptide in lipid, X_L, and in water, X_W,

$$\frac{I_t(\lambda)}{n_L + n_W} = X_L \Phi_L I_{L,N}(\lambda) + X_W \Phi_W I_{W,N}(\lambda) \quad \text{(AI.3)}$$

$I_t(\lambda)$, can be expressed in terms of the average quantum yield of peptide, $\langle \Phi \rangle_{L,W}$,

$$I_t(\lambda) = (n_L + n_W)\langle \Phi \rangle_{L,W} I_{t,N}(\lambda) \quad \text{(AI.4)}$$

$$\langle \Phi \rangle_{L,W} = X_L \Phi_L + X_W \Phi_W = (1 - X_W)\Phi_L + X_W \Phi_W \quad \text{(AI.5)}$$

Combining Eqs. (AI.3), (AI.4) and (AI.5):

$$I_{L,N}(\lambda) = \left(1 + \frac{X_W}{1 - X_W}\frac{\Phi_W}{\Phi_L}\right) I_{t,N}(\lambda) - \frac{X_W}{1 - X_W}\frac{\Phi_W}{\Phi_L} I_{W,N}(\lambda) \quad \text{(AI.6)}$$

Considering the Eq. (4) (see text),

$$\frac{X_W}{1 - X_W} \approx \frac{1}{K_p \gamma_L [L]} \quad \text{(AI.7)}$$

Therefore, the peptide emission spectrum when totally inserted in lipid membranes, is obtained,

$$I_{L,N}(\lambda) = \left(1 + \frac{1}{K_p \gamma_L [L]}\frac{\Phi_W}{\Phi_L}\right) I_{t,N}(\lambda) - \frac{1}{K_p \gamma_L [L]}\frac{\Phi_W}{\Phi_L} I_{W,N}(\lambda) \quad \text{(AI.8)}$$

Appendix B. Partition formalism accounting for self-quenching in membranes

The quantum yield of a fluorophore population is a linear combination of its components,

$$\Phi = X_L \Phi_L + X_W \Phi_W \quad \text{(AII.1)}$$

Eq. (4) (see text) can be applied to most experimental conditions (lipidic volume very small relative to the total sample volume, $\gamma_L[L] << 1$). Combining Eqs. (AII.1) and (4):

$$\Phi = \frac{\gamma_L K_p [L]}{1 + \gamma_L K_p [L]} \Phi_L + \frac{1}{1 + \gamma_L K_p [L]} \Phi_W \quad \text{(AII.2)}$$

Considering that there is no significant spectral shift influence on the measured fluorescence intensity, I:

$$I = \frac{\gamma_L K_p [L]}{1 + \gamma_L K_p [L]} I_L + \frac{1}{1 + \gamma_L K_p [L]} I_W \quad \text{(AII.3)}$$

where I_L is the emission intensity of the fluorophore molecules incorporated in lipid, in the case of self-quenching absence. I_L is constant if the fluorophore concentration is maintained throughout the experiment. In the case of existing self-quenching, I_L is dependent on lipidic concentration. When lipid concentration is low, the fluorophore concentration in the membrane is high, and the self-quenching notable. In the case of self-quenching, I_L is the intensity that would be recorded in case all fluorophores had the quantum yield of molecules incorporated in lipid at infinite dilution.

In homogeneous solution, *self-quenching* can be described by, [1]

$$\frac{1}{I} = \frac{k_f + k_{nr}}{I_{exc} \varepsilon l k_f [F]} + \frac{k_q}{I_{exc} \varepsilon l k_f} \quad \text{(AII.4)}$$

where I_{exc} is the excitation light intensity, k_q is the kinetic constant of the quenching process, k_f is the radiative fluorescence constant, and $[F]$ is the fluorophore concentration. Considering $k_1 = I_{exc} \Phi \varepsilon l$ and $k_2 = \frac{k_q}{k_f}\frac{1}{\varepsilon l}$, the fluorescence intensity of flurophore can be described by Eq. (AII.5),

$$I = \frac{k_1 [F]}{1 + k_2 k_1 [F]} \quad \text{(AII.5)}$$

In a partition experiment, self-quenching is a consequence of fluorophore compartmentalization inside the lipidic matrix. Imagining that all illuminated volume is occupied by lipidic matrix (limit condition for I_L) and that the lipidic concentration is constant, the fluorescence

intensity dependence on fluorophore concentration, $I_L([F])$ is dictated by Eq. (AII.5), where $[F]$ stands for the fluorophore concentration in the lipidic matrix ($[F]_L$).

In this limit situation, $[F]_L = n_t/v_t$, where n_t is the total number of solute moles and v_t is the total illuminated volume. However, in attainable experimental conditions, only a fraction of the lipid is being illuminated. This fraction equals the fraction of fluorophores being illuminated (n_i/n_t, where n_i and n_t are the illuminated and total moles of fluorophore, respectively). Thus,

$$I([L]) = \frac{k_1[F]_L}{1 + k_2 k_1 [F]_L} \frac{n_i}{n_t} = \frac{k_1[F]_t}{1 + k_2 k_1 [F]_L} \quad \text{(AII.6)}$$

($[F]_t$ is the fluorophore concentration over the whole volume). Taking Eq. (3) (see text), $[F]_L$ is related with $[F]_t$,

$$[F]_L = \frac{K_p}{1 + K_p \gamma_L [L]} [F]_t \quad \text{(AII.7)}$$

So, fluorescence intensity dependence on lipid concentration is:

$$I([L]) = \frac{k_1[F]_t}{1 + k_2 k_1 \dfrac{K_p[F]_t}{1 + k_p \gamma_L [L]}}$$

$$= k_1[F]_t \frac{1 + K_p \gamma_L [L]}{1 + K_p \gamma_L [L] + k_2 K_p k_1 [F]_t} \quad \text{(AII.8)}$$

$k_1[F]_t = I_L$ is the fluorescence emission intensity recorded in the absence of self-quenching, so,

$$I([L]) = I_L \frac{1 + K_p \gamma_L [L]}{1 + K_p \gamma_L [L] + k_2 K_p I_L} \quad \text{(AII.9)}$$

Combining Eqs. (AII.3) and (AII.9),

$$I = \frac{\gamma_L K_p [L] I_L}{1 + K_p \gamma_L [L] + k_2 K_p I_L} + \frac{I_W}{1 + \gamma_L K_p [L]} \quad \text{(AII.10)}$$

Appendix C. Kinetic of partition formalism

If the limit conditions are,

$$n_W(t = 0) = n_t, \quad n_L(t = 0) = 0$$

$$n_L(t = \infty) \approx \gamma_L [L] K_p n_W$$

$$0 < t < \infty \quad n_W(t) = n_t - n_L(t)$$

the fluorescence intensity dependence on time can be described by:

$$I(t) \propto \Phi_L n_L + \Phi_W n_W$$

$$I(t = 0) \propto \Phi_W n_t$$

$$0 < t < \infty$$

therefore,

$$\frac{I(t)}{I(t = 0)} = \frac{\Phi_L}{\Phi_W} \frac{n_L(t)}{n_t} + \frac{n_W(t)}{n_t} \quad \text{(AIII.1)}$$

The relative intensity, $I_R(t) = I(t) \neq I(t = 0)$, can be rewritten:

$$I_R(t) = \left(\frac{\Phi_L}{\Phi_W} - 1 \right) \frac{n_L(t)}{n_t} + 1 \quad \text{(AIII.2)}$$

At $t = \infty$,

$$\frac{n_L(t = \infty)}{n_W(t = \infty)} = \gamma_L [L] K_p \quad \text{(AIII.3)}$$

$$\frac{n_L(t = \infty)}{n_t - n_L(t = \infty)} = \gamma_L [L] K_p \quad \text{(AIII.4)}$$

$$\frac{n_L(t = \infty)}{n_t} = \frac{\gamma_L [L] K_p}{1 + \gamma_L [L] K_p} \quad \text{(AIII.5)}$$

K_p can be expressed in terms of kinetic constants,

$$K_p = \frac{k_{in}}{k_{out}} \quad \text{(AIII.6)}$$

where k_{in} and k_{out} are the first-order velocity constants of the fluorophore entering and leaving the lipidic matrix, respectively. Under the framework of our kinetic model, [2]

$$k_{in} t = \frac{n_L(t = \infty)}{n_t} \ln \left(\frac{n_L(t = \infty)}{n_t(t = \infty) - n_L(t)} \right) \quad \text{(AIII.7)}$$

Therefore,

$$\exp \left(k_{in} t \frac{n_t}{n_L(t = \infty)} \right) = \frac{n_L(t = \infty)}{n_t(t = \infty) - n_L(t)} \quad \text{(AIII.8)}$$

But

$$\frac{n_L(t)}{n_L(t = \infty)} = 1 - \exp \left(- \frac{n_t}{n_L(t = \infty)} k_{in} t \right) \quad \text{(AIII.9)}$$

combining Eq. (AIII.5) with Eq. (AIII.9),

$$\frac{n_L(t)}{n_t} = \frac{\gamma_L [L] K_p}{1 + \gamma_L [L] K_p} \left(1 - \exp \left(- \frac{n_t}{n_L(t = \infty)} k_{in} t \right) \right) \quad \text{(AIII.10)}$$

when this term is applied in Eq. (AIII.2),

$$I_R(t) = \left(\frac{\Phi_L}{\Phi_W} - 1 \right) \frac{\gamma_L [L] K_p}{1 + \gamma_L [L] K_p} \times \left(1 - \exp \left(- \frac{1 + K_p [L] \gamma_L}{\gamma_L [L] K_p} \right) k_{in} t \right) + 1 \quad \text{(AIII.11)}$$

References

[1] M.J.E. Prieto, M. Castanho, A. Coutinho, A. Ortiz, F.J. Aranda, J.C. Gómez-Fernández, Fluorescence study of a derivatized diacylglycerol incorporated in model membranes, Chem. Physics of Lipids 69 (1994) 75–85.

[2] K.J. Laider, Chemical Kinetics, 3rd Ed., Harper Collins Publishers, NY, 1987.

References

[1] J.S Wadia, M. Becker-Hapak, S.F. Dowdy, Protein transport, in: Ü. Langel (Ed.), Cell-Penetrating Peptides, Processes and Applications, CRC Press Pharmacology and Toxicology Series, CRC press, NY, 2002, pp. 365–375.
[2] A. Eguchi, T. Akuta, H. Okuyama, T. Senda, H. Yokoi, H. Inokuchi, S. Fujita, T. Hayakama, K. Takeda, M. Hasegawa, M. Nakanisshi, Protein transduction domain of HIV-1 Tat Protein promotes efficient delivery of DNA into mammalian cells, J. Biol. Chem. 247 (2001) 27205–27210.
[3] M.A. Bogoyevitch, T.S. Kendrick, C.H. Dominic, R.K. Barr, Taking the cell by stealth or storm? Protein transduction domain (PTDs) as versatile vectors for delivery, DNA Cell Biol. 21 (2002) 879–894.
[4] J.P. Richard, K. Melikov, E. Vives, C. Ramos, B. Verbeure, M.J. Gait, L.V. Chernomordik, B. Lebleu, Cell-penetrating peptides, a reevaluation of the mechanism of cellular uptake, J. Biol. Chem. 278 (2003) 585–590.
[5] S.R. Schwarze, K.A. Hruska, S.F. Dowdy, Protein transduction: unrestricted delivery into all cells? Trends Cell Biol. 10 (2000) 290–295.
[6] L. Chaloin, N.V. Mau, G. Divita, F. Heitz, Interactions of cell-penetrating peptides with membranes, in: Ü. Langel (Ed.), Cell-Penetrating Peptides, Processes and Applications, CRC Press Pharmacology and Toxicology Series, CRC press, NY, 2002, pp. 23–51.
[7] M.C. Morris, J. Depollier, J. Mery, F. Heitz, G. Divita, A peptide carrier for the delivery of biologically active proteins into mammalian cells, Nat. Biotechnol. 19 (2001) 1143–1147.
[8] http://www.activemotif.com/products/cell/chariot. php, 2004.
[9] C.M. Morris, L. Chalion, F. Heitz, G. Divita, Signal sequence-based cell-penetrating peptides and their applications for gene delivery, in: Ü. Langel (Ed.), Cell-Penetrating Peptides, Processes and Applications, CRC Press Pharmacology and Toxicology Series, CRC press, NY, 2002, pp. 93–113.
[10] A. Ikari, M. Nakano, K. Kawano, Y. Suketa, Up-regulation of sodium-dependent glucose transporter by interaction with heat shock protein 70, J. Biol. Chem. 277 (2002) 33338–33343.
[11] M. Coulpier, J. Anders, C.F. Ibáñez, Coordinated activation of autophosphorilation sites in the RET receptor tyrosine kinase, J. Biol. Chem. 277 (2002) 1991–1999.
[12] J. Zhou, J.-T. Hsieh, The inhibitory role of DOC-2/DAB2 in growth factor receptor mediated signal cascade, J. Biol. Chem. 276 (2001) 27793–27798.
[13] Y. Wu, M.D. Wood, F. Katagiri, Direct delivery of bacterial avirulence proteins into resistant *Arabidopsis* protoplasts leads to hypersensitive cell death, Plant J. 33 (2003) 131–137.
[14] M. Morris, V. Robert-Hebmann, L. Chaloin, J. Mery, F. Heitz, C. Devaux, R.S. Goody, G. Divita, A new potent HIV-1 reverse transcriptase inhibitor, J. Biol. Chem. 274 (1999) 24941–24946.
[15] L. Chaloin, N.V. Mau, G. Divita, F. Heitz, Interactions of cell-penetrating peptides with membranes, in: Ü. Langel (Ed.), Cell-Penetrating Peptides, Processes and Applications, CRC Press Pharmacology and Toxicology Series, CRC press, NY, 2002, pp. 163–186.
[16] D. Terrone, S.L. W. Sang, L. Roudaia, J.R. Silvius, Penetratin and related cell-penetrating cationic peptides can translocate across lipid bilayers in the presence of transbilayer potential, Biochemistry 42 (2003) 13787–13799.
[17] S.T. Henriques, M.A.R.B. Castanho, Consequences of nonlytic membrane perturbation to the translocation of the cell penetrating peptide pep-1 in lipidic vesicles, Biochemistry 43 (2004) 9716–9724.
[18] S. Deshayes, A. Heitz, M.C. Morris, P. Charnet, G. Divita, F. Heitz, Insight into the mechanism of internalization of the cell-penetrating carrier peptide pep-1 through conformational analysis, Biochemistry 43 (2004) 1449–1457.
[19] G.A. Caputo, E. London, Using a novel dual fluorescence quenching assay for measurement of tryptophan depth within lipid bilayers to determine hydrophobic α-helix location within membranes, Biochemistry 42 (2003) 3265–3274.
[20] N.C. Santos, M.A.R.B. Castanho, Fluorescence spectroscopy methodologies on the study of proteins and peptides. On the 150th anniversary of protein fluorescence, Trends Appl. Spectrosc. 4 (2002) 113–125.
[21] N.C. Santos, M.A.R.B. Castanho, Teaching light scattering spectroscopy: the dimension and shape of tobacco mosaic virus, Biophys. J. 71 (1996) 1641–1650.
[22] A. Coutinho, M. Prieto, Ribonuclease T1 and alcohol dehydrogenase fluorescence quenching by acrylamide, J. Chem. Educ. 70 (1993) 425–428.
[23] J.R. Lakowics, Principles of Fluorescence Spectroscopy, 2nd ed., Kluwer Academic/Plenum publishers, NY, 1999.
[24] T. Wieprecht, M. Beyermann, J. Seeling, Thermodynamics of the coli-α-helix transition of amphipathic peptides in a membrane environment; the role of the curvature, Biophys. Chem. 96 (2002) 191–201.
[25] L.D. Mayer, M.J. Hope, P.R. Cullis, Vesicles of variable sizes produced by a rapid extrusion procedure, Biochim. Biophys. Acta 858 (1986) 161–168.
[26] N.C. Santos, M. Prieto, M.A.R.B. Castanho, Quantifying molecular partition into model systems of biomembranes: an emphasis on optical spectroscopic methods, Biochim. Biophys. Acta 1612 (2003) 123–135.
[27] S.W. Chiu, E. Jakobsson, S. Subramanian, H.L. Scott, Combined Monte Carlo and molecular dynamics simulation of fully hydrated dioleyl and palmitoyl-oleyl-phosphatidylcholine lipid bilayers, Biophys. J. 77 (1999) 2462–2469.
[28] J.F. Naigle, M.C. Weiner, Structure of fully hydrated bilayer dispersions, Biochim. Biophys. Acta 942 (1988) 1–10.
[29] N.C. Santos, M. Prieto, M.A.R.B. Castanho, Interaction of the major epitope of HIV gp41 with membrane novel systems. A fluorescence spectroscopy study, Biochemistry 37 (1998) 8674–8682.
[30] M.X. Fernandes, J.G. Torre, M.A.R.B. Castanho, Joint determination by brownian dynamics and fluorescence quenching of the in-depth location profile of biomolecules in membranes, Anal. Biochem. 307 (2002) 1–12.
[31] J.R. Wardlaw, W.H. Sawyer, K.P. Ghiggino, Vertical fluctuations of phospholipid acyl chains in bilayers, FEBS Lett. 223 (1987) 20–24.
[32] S.E. Harding, D.B. Sattelle, V.A. Bloomfield (Eds.), Laser Light Scattering in Biochemistry, Royal Soc. Chemistry, Cambridge, 1992.
[33] M. Castanho, W. Brown, M. Prieto, Filipin and its interaction with cholesterol in aqueous media studied using static and dynamic light scattering, Biopolymers 34 (1994) 447–456.
[34] C. Mangavel, R. Maget-Dana, P. Tauc, J.-C. Brochon, D. Sy, A. Reynaud, Structural investigations of basic amphipathic model peptides in the presence of lipid vesicles studied by circular dichroism, fluorescence monolayer and modelling, Biochim. Biophys. Acta 1371 (1998) 265–2983.
[35] L.A. Falls, B.C. Furie, M. Jacobs, B. Furie, A.C. Rigby, The ω-loop region of the human prothrombin γ-carboxyglutamic acid domain penetrates anionic phospholipid membranes, J. Biol. Chem. 276 (2001) 23895–23902.
[36] J.R. Silvius, Lipidated peptides as tools for understanding the membrane interactions of lipid-modified proteins, in: S.A. Simon, T.J. McIntosh (Eds.), Peptide–Lipid Interactions, Academic Press, California, 2002, pp. 371–395.
[37] D. Murray, A. Arbuzova, B. Honig, S. McLaughlin, The role of electrostatic and nonpolar interactions in the association of peripheral proteins with membranes, in: S.A. Simon, T.J. McIntosh

(Eds.), Peptide–Lipid Interactions, Academic Press, California, 2002, pp. 277–307.
[38] R.B. Gennis, Biomembranes, Molecular Structure and Function, Springer-verlag, NY, 1989.
[39] C.E. Dempsey, S. Ueno, M. Avison, Enhanced membrane permeabilization and antibacterial activity of a disulfide–dimerized magainin analogue, Biochemistry 42 (2003) 402–409.
[40] K. Simons, E. Ikonen, Functional rafts in cell membranes, Nature 387 (1997) 569–572.
[41] C.R. Mateo, J.-C. Brochon, M.P. Lillo, A.U. Acuña, Liquid-crystalline phases of cholesterol/lipid bilayers as revealed by the fluorescence of *trans*-parinaric acid, Biophys. J. 65 (1993) 2237–2247.
[42] J.R. Silvius, Role of cholesterol in lipid raft formation: lessons from lipid model systems, Biochim. Biophys. Acta 1610 (2003) 174–183.
[43] S. Lehrer, Solute perturbation of protein fluorescence. The quenching of the tryptophyl fluorescence of model compounds and of lysozyme by iodide ion, Biochemistry 10 (1971) 3254–3263.